RSC Advances




ROYAL SOCIETY OF CHEMISTRY

www.rsc.org/advances

# New insights in partial nitrification start-up revealed by model based approach

**Jun Wu*, Gang Yan, Guojing Zhou, Ting Xu**

School of Environmental Engineering and science, Yangzhou University, 196 West Huayang Road, Yangzhou, Jiangsu, 225127, China. Tel: +86-514-87971389, Fax: +86-514-87978626, Email address: j.wu@yzu.edu.cn

*Correspondence author

## Abstract

New insight in partial nitrification was revealed by using a model based approach to study the synergetic impact of various factors on partial nitrification. The traditional argument for using low DO (dissolved oxygen) in achieving partial nitrification is that AOB (ammonium oxidizing bacteria) has higher DO affinity than NOB (nitrite oxidizing bacteria). However, the AOB was found to have lower DO affinity (DO half saturation constant $K_{O,AOB}$ =1.0 mg/L) than NOB ($K_{O,NOB}$ =0.35 mg/L) in the nitrification process in this study. The rational for using low DO concentration in this study was to slow down the ammonium removal, therefore increase the FA (free ammonia) concentration for the inhibition of NOB. The optimal operational strategy for partial nitrification start-up was identified by the model based approach to be at sludge retention time of 10 days, DO at 1.0 mg/L and pH at 8.2. The results indicated that nitrite accumulation rate of above 80% and complete ammonium removal can be achieved within 10 days of startup period by applying the model based optimization results.

**Keywords:** Model based optimization; partial nitrification; free ammonia**;** biological nitrogen removal; DO affinity

## Introduction

The traditional biological nitrogen removal (BNR) is achieved by nitrification (ammonium ($NH_4^+$) to nitrate ($NO_3^-$)) and de-nitrification (nitrate $NO_3^-$ to $N_2$ gas)[1]. The complete nitrification can be described by a two-step process, with the first conversion of the ammonium ($NH_4^+$) into nitrite ($NO_2^-$) by ammonium oxidizing bacteria (AOB) and subsequent nitrite into nitrate ($NO_3^-$) by nitrite oxidizing bacteria (NOB)[2]. Compared to the complete nitrification, the partial nitrification provides a shortcut for biological nitrogen removal. Significant reduction in oxygen supply and carbon source has been reported [3].

Partial nitrification is usually achieved by inhibiting the growth of NOB or completely washout of NOB[4]. A number of factors can affect the AOB and NOB growth conditions including temperature, pH, dissolved oxygen (DO) concentration, free ammonium (FA) concentration or addition of chemicals for inhibition of nitrification[5-12].

Applying low DO concentration is one of the most widely used techniques for partial

nitrification start-up [8, 13, 14]. One of the common explanations for using low DO concentration is that NOB has lower DO affinity (higher DO half saturation constant) than AOB[9, 15]. Therefore, NOB will be wash-out under DO limitations. However, study by Balmelle et al. [16] has shown that DO concentration between 0.5-8.0 mg/L has no effect on the build-up of nitrite and the $NH_4^+$ removal rate was significantly reduced at lower DO. Nitrite build-up up to 300 mg /L were obtained in an upflow submerged filter at DO concentrations of 4–5 mg /L under $NH_4^+$ load rate of 1 g $NH_4^+$ /($m^2$*d)[17]. A large variety of SRT and temperature have been used for partial nitrification operation as well [5, 9, 18].

The high FA concentration was found to be inhibitive to both AOB and NOB[19, 20]. For domestic wastewater, the FA concentration is usually not high enough for AOB inhibition[21]. However, there are few consensuses on the exact FA concentration that will cause NOB inhibition. NOB inhibition by FA concentration of 6-11mg N-$NH_3$ /L has been reported [22, 23]. However, Anthonisen et al. [19] and Jubany et al.[9] reported the inhibitive FA concentration was within 0.1-1.0 mg N-$NH_3$ /L.

The conflicting conditions for achieving nitrite build-up suggests that partial nitrification performance is affected by many interacting factors[24]. A systematic approach that considers the synergetic impact of the major factors for partial nitrification should be developed. Mathematical models are powerful tools for elucidating process mechanisms. Although several models have been developed to simulate partial nitrification [9, 22, 25-27], no consistent explanation for the conflicting conditions in achieving partial nitrification has been suggested. This is probably because the critical parameter values used in these models were taken from other studies that might have different experimental conditions.

Based on the fully calibrated model, the optimal condition for partial nitrification can be calculated. The minimum solid retention time (SRT) required for sustaining bacteria growth is governed by the following inequality:

$$SRT \geq \frac{1}{\mu - b} \quad (1)$$

Where, $\mu$ is the maximum specific growth rate ($d^{-1}$), $b$ is the decay rate ($d^{-1}$). For successful partial nitrification operation, the SRT needs to satisfy the following inequality:

$$\frac{1}{\mu_{NOB} - b_{NOB}} \geq SRT \geq \frac{1}{\mu_{AOB} - b_{AOB}} \quad (2)$$

Where $\mu_{AOB}$ *and* $\mu_{NOB}$ is the specific growth rate ($d^{-1}$) for AOB and NOB respectively, $b_{AOB}$ *and* $b_{NOB}$ is the decay rate ($d^{-1}$) for AOB and NOB respectively. The biomass growth and decay are affected by a number of factors including temperature, DO and FA concentration etc. With the aid of the full calibrated model, the optimal condition for partial nitrification can be calculated.

In summary, the study tried to offer new insights in partial nitrification by considering the synergetic impacts of various factors and suggest a rapid partial nitrification start-up method based on the model based approach.

## 2 Material and method

### 2.1 Experimental sequencing batch reactor

The SBR (sequencing batch reactor) with 8 L effective volume was operated periodically at 30 minutes settlement, 15 minutes of discharging and filling, 2 hours of anoxic reaction and 3 h of aerobic phase. The SBR was placed in air conditioned room with temperature controlled at 20℃. The SBR was initially operated at complete nitrification mode for 30 days, during which the SRT, DO and pH were controlled at 15 days, 3 mg/L and 6.8-7.5 respectively. Then, the complete nitrification was converted to partial nitrification by applying operational conditions derived from model based optimization.

The influent $NH_4^+$, organic carbon source and phosphorous were prepared by addition of $NH_4Cl$ , acetate and $KH_2PO_4$ to achieve N-$NH_4^+$, COD (chemical oxygen demand) and TP (Total Phosphorous) concentration of 128.0±3.6mg/L, 500.0±26.8mg/L and 5.0±0.6mg/L respectively. Other trace elements were added according to the recipe by Wu et al. [28]. The 15 minutes of discharging and filling allows 2.5L liquid in the reactor to be replaced, which resulted in the initial N- $NH_4^+$ concentration to be around 40.0 ±1.8 mg/L. The nitrogen load was at 0.325 kg N-$NH_4^+$/($m^3$*d). $NaHCO_3$ and HCl were used for pH adjustment to the desired range.

The SBR operation was controlled by a data acquisition broad USB-6009 (NI) connected to computer using MATLAB ® 7.0 software. The DO was measured by HACH LDO oxygen probe. A mechanical stirrer was installed for the mixing in the anoxic and aerobic phase. The aeration was achieved by using air pump with variable airflow rate to achieve desired DO concentration within less than ±0.1 mg/L error.

### 2.2 Mathematical model for nitrification

The mathematical model for nitrification was modified from literatures [22, 26]. The model matrix and parameter definition were shown in **Table 1** and **Table 2**. Due to the low $NH_4^+$ concentration, the total ammonium nitrogen (TAN = N-$NH_3$+ N-$NH_4^+$) was used as substrate for AOB to produce better fit between the experimental and simulated data. The FA and $HNO_2$ inhibition to AOB was ignored as their concentration in the SBR was much lower than the commonly assumed inhibition threshold value[21]. A Monod-term was used to simulate the DO limitation on both AOB and NOB. The FA inhibition on NOB was modeled by an inverse Monod term. The FA concentration was calculated by the following equation[29]:

$$FA = \frac{S_{TAN} 10^{pH}}{e^{\frac{6344}{273+T}}} \quad (3)$$

Where, $S_{TAN}$ is the TAN concentration, T is the temperature.

In the tradition activated sludge models (ASM), the same yield coefficient and decay rate were used for AOB and NOB [30]. In this study, different yield values were uniquely determined for AOB and NOB.

### 2.3 Model parameter estimation

The majority of parameters shown in **Table 2** were estimated by by respirometric method adapted from Vanrolleghem et al. [31]. The oxygen uptake rate (OUR) was measured by the respirometer described in [32]. As the determination of some parameters depends on the known value of other parameters, the parameter estimation was carried out strictly with the following order:

*1)* $Y_{NOB}$

$Y_{NOB}$ was determined by addition of a certain volume of N-$NO_2^-$ solution to the respirometer chamber to reach N-$NO_2^-$ concentration of around10 mg/L. The biomass in the respirometer was aerated overnight to reach endogenous respiration stage beforehand. The OUR was monitored every 5 minutes after $NO_2^-$ addition until it reached endogenous respiration again. The DO was maintained at above 5 mg/L during the OUR test.

The total oxygen consumed in oxidation of $NO_2^-$ to $NO_3^-$ by NOB ($\int OUR_{NOB}$) was calculated by subtracting the endogenous respiration oxygen consumption ($\int OUR_{end}$) from the total oxygen consumption after $NO_2^-$ addition ($\int OUR_{NO}^{T}$) (Equation (4)).

$$\int OUR_{NOB} = \int OUR_{NO}^{T} - \int OUR_{end} \quad (4)$$

The $Y_{NOB}$ can be calculated by the following equation:

$$Y_{NOB} = \frac{1.14 S_{NO2} - \int OUR_{NOB} dt}{S_{NO2}} \quad (5)$$

Where, $S_{NO2}$ is the added N-$NO_2^-$ concentration (10 mg/L)

*2)* $Y_{AOB}$

Immediately after the biomass reached endogenous respiration after the previous $Y_{NOB}$ test experiment, N-$NH_4^+$ was added at 10 mg/L. The OUR was recorded until it reached endogenous respiration. The oxygen consumed in oxidation of $NH_4^-$ to $NO_2^-$ by AOB

($\int OUR_{AOB}$) was calculated by subtracting the oxygen consumption after $NO_2^-$ addition ($\int OUR_{NO}^T$) from the oxygen consumption after $NH_4^-$ addition ($\int OUR_{NH}^T$) (Equation(6)).

$$\int OUR_{AOB} = \int OUR_{NH}^T - \int OUR_{NO}^T \quad (6)$$

The $Y_{AOB}$ can be calculated by the following equation:

$$Y_{AOB} = \frac{3.43\, S_{NH} - \int OUR_{AOB}\, dt}{S_{NH}} \quad (7)$$

Where, $S_{NH}$ is the added N-$NH_4^-$ concentration (10 mg/L)

*3)* $K_{NO2}$

Using the same OUR data for $Y_{NOB}$ measurement, the parameter $K_{NO2}$ can be estimated. As there was no DO limitation and FA inhibition, the simulated $OUR_{NOB}$ can be expressed by the following equation:

$$OUR_{NOB} = (1 - \frac{1.14}{Y_{NOB}})\mu_{NOB} X_{NOB} \frac{S_{NO2}}{K_{NO2} + S_{NO2}} \quad (8)$$

The consumption of $NO_2^-$ can be expressed by the following equation:

$$\frac{dS_{NO2}}{dt} = -\frac{1}{Y_{NOB}} \mu_{NOB} X_{NOB} \frac{S_{NO2}}{K_{NO2} + S_{NO2}} \quad (9)$$

As the initial concentration was known and $Y_{NOB}$ was previously determined, the $K_{NO2}$ and $\mu_{NOB}X_{NOB}$ combination can be estimated by curve fitting the simulated $OUR_{NOB}$ (Equation(8)) to the experimentally determined OUR.

*4)* $K_{NH}$

The exogenous OUR after addition of N-$NH_4^-$ can be simulated by the following equation

$$OUR_{NH} = (1 - \frac{3.43}{Y_{AOB}})\mu_{AOB} X_{AOB} \frac{S_{NH}}{K_{NH} + S_{NH}} + (1 - \frac{1.14}{Y_{NOB}})\mu_{NOB} X_{NOB} \frac{S_{NO2}}{K_{NO2} + S_{NO2}} \quad (10)$$

The consumption of TAN can be expressed by the following equation

$$\frac{dS_{TAN}}{dt} = -(\frac{1}{Y_{AOB}} - i_{XB})\mu_{AOB} X_{AOB} \frac{S_{TAN}}{K_{NH} + S_{TAN}} \quad (11)$$

Combining equation (9), (10)and (11), the simulated exogenous OUR can be calculated. By curve fitting the simulated exogenous OUR to the measured OUR in $Y_{AOB}$ measurement, the $K_{NH}$ and $\mu_{AOB}X_{AOB}$ combination can be estimated. Because the $i_{xb}$ value is a very small, its value won't affect model prediction. Therefore the $i_{xb}$ value was taken from Henze et al. [33].

5) $K_{O,AOB}$ and $K_{O,NOB}$

$K_{O,AOB}$ and $K_{O,NOB}$ were determined by measuring the $NH_4^+$ and $NO_2^-$ removal rates at various DO concentration, provided that other conditions were kept constant.

6) $b_{AOB}$ and $b_{NOB}$

For AOB and NOB under endogenous respiration rate, there change could be simulated by the following equation:

(12) $$\frac{dX_{AOB}}{dt} = -b_{AOB}X_{AOB}$$

(13) $$\frac{dX_{NOB}}{dt} = -b_{NOB}X_{NOB}$$

The above two equations can be converted into:

(14) $$\frac{X_{AOB}(t)}{X_{AOB}^0} = e^{-tb_{AOB}}$$

(15) $$\frac{X_{NOB}(t)}{X_{NOB}^0} = e^{-tb_{NOB}}$$

Where $X_{AOB}^0$ and $X_{NOB}^0$ initial AOB and NOB concentration, $X_{AOB}(t)$ and $X_{NOB}(t)$ are the AOB and NOB concentration at time t.

According to the equation (8) and (10), the OUR value after addition of the same amount of $NH_4^+$ and $NO_2^-$ was proportional to the AOB and NOB concentration. The equation (14) and (15) can be changed to:

(16) $$\frac{OUR_{NH}(t)}{OUR_{NH}^0} = e^{-tb_{AOB}}$$

(17) $$\frac{OUR_{NO2}(t)}{OUR_{NO2}^0} = e^{-tb_{NOB}}$$

For the measurement of $b_{AOB}$ and $b_{NOB}$, the biomass was continuously aerated for more than 8 days. A small spike of $NH_4^+$ and $NO_2^-$ of 3mg/L was added to measure exogenous $OUR_{NH}$ and $OUR_{NO2}$ each day. The small amount of added $NH_4^+$ and $NO_2^-$ was to make sure that the biomass concentration was not significantly changed by the $NH_4^+$ and $NO_2^-$ addition.

7) $\mu_{AOB}$ and $\mu_{NOB}$

The $\mu_{AOB}$ and $\mu_{NOB}$ were measured by OUR measurement at high Food to Mass (F/M) ratio. $N\text{-}NH_4^+$ of 60mg/L were added to the respirometer with biomass concentration of around 50 mg VSS/L to produce an unlimited growth environment for AOB, in which the exogenous $OUR_{NH}$ can be expressed by the following equation:

$$\frac{OUR_{NH}(t)}{OUR_{NH}^0} = e^{t(\mu_{AOB} - b_{AOB})} \quad (18)$$

Similarly, the $\mu_{NOB}$ was estimated by measuring $OUR_{NO2}$ with addition of 60 mg/L of $N\text{-}NO_2^-$ using the following equation:

$$\frac{OUR_{NO2}(t)}{OUR_{NO2}^0} = e^{t(\mu_{NOB} - b_{NOB})} \quad (19)$$

Both $b_{AOB}$ and $b_{NOB}$ were previously determined.

*8)* $K_I$

The $K_I$ was estimated by operating the SBR reactor at pH =7.5 and pH = 8.0. The $NH_4^+$, $NO_3^-$and $NO_2^-$ concentration in the SBR were measured every 15 minutes. The $K_I$ value were adjusted until a good fit between the measured and simulated $NH_4^+$ , $NO_3^-$and $NO_2^-$ data. For the model simulation, the previous determined parameter values were used.

**2.4 Model based optimization strategy for partial nitrification**

The optimization strategy is to search for the optimal operation condition that could produce the required TAN removal rate and nitrite accumulation rate ($NO_2^-$/( $NO_3^-$+ $NO_2^-$)) within the shortest startup period. The operation condition includes pH, DO set point and SRT. The hydraulic retention time (HRT) and nitrogen load is fixed due the SBR configuration. The optimization toolbox within MATLAB 7.0 software was used for the optimization process. The global optimal solution for the optimization problem that involves highly non-linear model equations in **Table 1** does not always exist. To reduce the complexity of the optimization problem, the pH was maintained at 8.2, which is within the optimal range of 7.5-8.6 reported by Ciudad et al. [34]. The pH value fixed at 8.2 was also because the de-nitrification step could usually increase pH to 8.0-8.2 and minimal alkalinity addition could be achieved during nitrification step.

The optimization problem was posed as:

$$f(SRT, DO) \quad (20)$$

Subject to:

$$S_{TAN}^{out} \le 0.1 mg/L \quad (21)$$

(22) $$\frac{S_{NO2}^{out}}{S_{NO2}^{out} + S_{NO3}^{out}} \geq 80\%$$

The optimization problem search for SRT and DO combinations that meets the above constraints of effluent TAN less than 0.1 mg/L and nitrite accumulation rate greater than 80%. The simulation time scale was set to be 5 times of the SRT to allow for the steady condition to be reached. An exhaustive search method enumerating all possible combinations of SRT and DO (SRT between 3 -15 days, DO between 0.4-5 mg/L) and checking whether each combination satisfies the constraints was used for solving the optimization problem. It should be noted there might exist more than one unique solution to the optimization problem as various combinations of SRT and DO could satisfy the constraints. The MATLAB 7.0 software was used for the calculation.

## 3. Results

### 3.1 Parameter calibration and verification

#### 3.1.1 Estimation of $Y_{AOB}$ , $Y_{NOB}$ , $K_{NO}$ and $K_{NH}$

**Fig.S1 (in the supporting information)** shows the exogenous OUR profile after addition of 9.8±0.4 mg/L of N-$NH_4^+$ (**Fig.S 1(1)**), and 9.6 ±0.4 mg/L of N- $NO_2^-$ (**Fig.S 1(2)**). By integrating the exogenous OUR curves over time, the total oxygen consumption due to $NH_4^+$ and $NO_2^-$ oxidation can be estimated. Using equation (5) and (6), the $Y_{AOB}$ and $Y_{NOB}$ were estimated to be 0.20±0.076 and 0.053±0.012 based on three repeated measurements. The $Y_{AOB}$ value determined is similar to the default autotrophic biomass yield in activated sludge model No.1 (ASM1) [33]. The $Y_{AOB}$ and $Y_{NOB}$ value used by[18]was 0.15 g COD/g N-$NH_4^+$ and 0.041 g COD/g N- $NO_2^-$ respectively.[35] has reported the $Y_{AOB}$ and $Y_{NOB}$ value at 0.18 g COD/g N-$NH_4^+$ and 0.06 g COD/g N- $NO_2^-$. The difference in the reported yield coefficients might due to different biomass origins and plant configurations. The calibration of yield coefficients allows the biomass production to be more precisely determined.

Using the same OUR curves for $Y_{AOB}$ and $Y_{NOB}$ measurement, affinity constant for N-$NH_4^+$ and N- $NO_2^-$ were calculated to be 0.51 mg/L N-$NH_4^+$ and 0.48 mg/L N- $NO_2^-$ respectively, which were similar to the default value by [33].

#### 3.1.2 Estimation of DO affinity constant ($K_{OAOB}$ and $K_{ONOB}$)

**Fig.S2** shows the air pump speed required to maintain the desired DO concentration of 0.5, 1.0 and 1.5 mg/L during oxidation of N- $NO_2^-$ (**Fig.S2(1-3)**)and N-$NH_4^+$ (**Fig.S2(4-6)**) at the same initial biomass and substrate concentration. The air pump speed was adjusted by the PID controller to maintain the desired DO concentration. The sudden drop of air pump speed indicated the completion of substrate oxidation. Therefore, if the same known initial substrate was added, the substrate consumption rate can be calculated. The time required for oxidation of 10 mg/L N- $NO_2^-$ at 0.5, 1.0 and 1.5 mg/L DO concentration was 1.2, 0.95 and 0.96 hour. In comparison, the correspondent time required for oxidation of 10 mg/L N-$NH_4^+$ was 2.8, 1.2

and 0.9 hour. This suggests that oxidation of N-$NH_4^+$ is more affected by DO concentration than the oxidation of N- $NO_2^-$. The DO affinity constant for AOB is higher than for NOB. By measuring the N-$NH_4^+$ and N- $NO_2^-$ removal rate at different DO concentration, the DO affinity constant for AOB and NOB ($K_{OAOB}$ and $K_{ONOB}$) can be measured at 1.0 and 0.35 mg $O_2$/L respectively (**Fig.S3**). The DO affinity values contradict to the commonly used DO affinity values for AOB and NOB[15, 21], which were the justification for choosing low DO condition to promote partial nitrification[8, 13]. However, the result is consistent with reports by[36, 37], in which the $K_{OAOB}$ value was shown to be higher than $K_{ONOB}$. Ciudad et al. [34] also reported that N-$NH_4^+$ removal rate was significantly dependent on the DO concentration, suggesting high $K_{OAOB}$ value. The conflicting reporting on the value $K_{OAOB}$ and $K_{ONOB}$ value indicates that controlling DO at lower value cannot always guarantee successful partial nitrification startup. A specific evaluation on the major factors affecting the AOB and NOB growth should be carried out for partial nitrification startup in different situations.

### 3.1.3 Estimation biomass decay rate ($b_{AOB}$ and $b_{NOB}$)

**Fig.S4** shows the exogenous $OUR_{NH}$ and $OUR_{NO2}$ after addition of 3mg/L of $NH_4^+$ and $NO_2^-$ respectively to endogenous respiration biomass. By curve fitting the measured data with equation (16) and (17), the $b_{AOB}$ and $b_{NOB}$ can be estimated at 0.13 and 0.05 $d^{-1}$ respectively. [38] have reported the $b_{AOB}$ at 0.4, probably due to the high DO (7 mg/L) and temperature (30 ℃) used in their test. The $b_{NOB}$ is also smaller than reported by Jubany et al. [39].

### 3.1.4 Estimation maximum specific growth rate ($\mu_{AOB}$ and $\mu_{NOB}$)

The $\mu_{AOB}$ and $\mu_{NOB}$ were estimated by measuring the $OUR_{NH}$ and $OUR_{NO2}$ under high F/M ratio (**Fig.S5**). The curve fitting the measured OUR with equation (18) and (19), the $\mu_{AOB}$ and $\mu_{NOB}$ were estimated at 0.74 and 0.68 $d^{-1}$ respectively. The $\mu_{AOB}$ and $\mu_{NOB}$ were reported to be 1.96 and 0.672 $d^{-1}$ by Pambrun et al. [22]. The difference can be explained by the high temperature used in their test. The method used in this study for $\mu_{AOB}$ and $\mu_{NOB}$ estimation does not need prior knowledge of AOB and NOB concentration. Therefore it is less prone to measurement errors.

### 3.1.5 Estimation of free $NH_3$ inhibition factor ($K_I$) for NOB

Two batch tests, with the same initial AOB, NOB and N-$NH_4^+$ concentration, but different pH value of 7.5±0.1 and 8.0±0.1, were used for estimation of $K_I$ value. **Fig. 1(1-2)** and **Fig.1(3-4)** show the profile of N-$NH_4^+$, N- $NO_2^-$ , N- $NO_3^-$, and FA under pH of 7.5±0.1 and 8.0±0.1 respectively. The FA was higher and the NOB was more inhibited under pH = 8.0±0.1 than pH = 7.5±0.1, indicated by higher N- $NO_2^-$ concentration. By curve fitting the measured N-$NH_4^+$, N- $NO_2^-$ and N- $NO_3^-$ concentration using nitrification model with parameters calibrated above, the $K_I$ value was estimated to be 0.33 mg N-$NH_3$ /L. A large variety of $K_I$ value can be found in the literature. The $K_I$ value estimated in this study is significantly lower than the $K_I$ value (6-11mg N-$NH_3$ /L) reported by Mauret et al. [23]and Pambrun et al. [22]. However, it is consistent with Anthonisen et al. [19] who observed that NOB could be inhibited

at FA concentration of 0.1-1.0 mg $N\text{-}NH_3$ /L. Jubany et al. [39] reported the $K_I$ value to be 0.95 mg $N\text{-}NH_3$ /L.

### 3.2 Model prediction results

By using the fully calibrated model, the possible outcome of different operation scenarios can be predicted without actually carrying out the experiments. **Fig.2** shows the predicted 3D plot of AOB, NOB, effluent $N\text{-}NH_4^+$ concentration and nitrite accumulation rate under different combinations of SRT and DO concentration. In general, high SRT and DO concentration produced more AOB and NOB. (**Fig.2(1-2)**) indicated that the SRT and DO concentration can be manipulated for NOB washout while retaining enough AOB for $N\text{-}NH_4^+$ removal. **Fig.2(3-4)** shows that the low effluent $N\text{-}NH_4^+$ concentration and high nitrite accumulation rate can be achieved by using appropriate SRT and DO combination.

**Fig.2(3-4)** also shows that partial nitrification can be achieved in nearly all the DO and SRT range investigated. The large variety of DO and SRT for partial nitrification startup might explain the contradict conditions reported in the experimental studies for partial nitrification[4].

**Fig.3(1)** shows the predicted AOB and NOB concentration under various DO concentration and SRT of 10 days. It can be seen that for DO less than 1.1 mg/L, complete washout of NOB can be expected. Above DO concentration of 0.95 mg/L, AOB can reach its highest steady state value. The effluent $N\text{-}NH_4^+$ concentration and nitrite accumulation rate under various DO concentration and SRT of 10 days were shown in **Fig.3(2).** If the treatment objective is to achieve effluent $N\text{-}NH_4^+$ concentration at near zero and PN rate of 80%, the DO concentration should be set between 0.9-1.35 mg/L. Similarly, under SRT of 15 days, to achieve the same treatment objective, lower and narrower DO range of 0.6-0.75 mg/L should be used (**Fig.4**). The narrow DO range at SRT = 15 days allows less room for DO control error. To increase reliability, the SRT = 10 days and DO = 1.2 mg/L combination were used for partial nitrification startup.

The initial AOB and NOB concentration ($AOB_0$ and $NOB_0$) also affected the startup of partial nitrification. Three hypothetical AOB and NOB initial concentration combinations ($AOB_0$=150mg/L, $NOB_0$ =50mg/L; $AOB_0$=75mg/L, $NOB_0$ =25mg/L; $AOB_0$=37.5mg/L, $NOB_0$ =12.5mg/L) were used to test their partial nitrification startup performance under SRT = 10 days and DO = 1.2 mg/L. Under high $AOB_0$ of 150mg/L and $NOB_0$ of 50mg/L, it will take a long time to achieve NOB washout (**Fig.5(1)**) and high nitrite accumulation rate (**Fig.5(3)**). However, the 100% removal of $N\text{-}NH_4^+$ was achieved quickly. On the contrary, NOB washout and high nitrite accumulation rate was achieved quickly under low initial $AOB_0$=37.5mg/L and $NOB_0$ =12.5mg/L condition. However, it will take long time to achieve high $N\text{-}NH_4^+$ removal rate. The $AOB_0$=37.5mg/L and $NOB_0$ =12.5mg/L combination provided a balance between NOB washout and $N\text{-}NH_4^+$ removal. Therefore, to achieve a fast conversion of the full nitrification process into a partial nitrification process, the initial biomass concentration should be adjusted carefully. In this study, the biomass from the full nitrification operation was diluted in half for the startup of partial nitrification.

### 3.3 Verification of the model based optimization results

The biomass from the previous full nitrification SBR reactor was diluted in half and used for the startup of partial nitrification operated under optimized SRT of 10 days and DO concentration of 1.2 mg/L. The AOB and NOB concentration were determined by measuring the exogenous $OUR_{NH}$ and $OUR_{NO2}$ and calculated using the known parameter values shown in **Table 2**. The $OUR_{NH}$ and $OUR_{NO2}$ were measured without substrate limitations. The pH value was controlled at 8.5 to prevent the second step nitrification for the $OUR_{NH}$ measurement. Therefore the AOB and NOB concentration can be calculated by equation (23) and (24).

(23) $$X_{NOB} = \frac{OUR_{NO2}}{(1-\frac{1.14}{Y_{NOB}})\mu_{NOB}}$$

(24) $$X_{AOB} = \frac{OUR_{NH}}{(1-\frac{3.43}{Y_{AOB}})\mu_{AOB}}$$

**Fig.6(1)** shows that the growth of AOB was significant while the NOB growth was inhibited. AOB dominance of 90% was achieved within 10 days of startup. The measured effluent $N\text{-}NH_4^+$ concentration was high initially (at 18 mg/L) due to the dilution of biomass. It decreased to near zero within 10 days due to the increase of AOB. The $N\text{-}NO_2^-$ concentration increased from around 20 mg/L to 32 mg/L in 10 days. The final nitrite accumulation rate stabilized at 80% after 10 days of startup period. The $N\text{-}NO_3^-$ concentration was below 9 mg/L throughout the experiment, suggesting that the growth of NOB was inhibited (**Fig.6(2)**). The partial nitrification was successfully started within days by applying the optimized operation conditions.

By using the parameters values shown in **Table 2** and the initial AOB and NOB concentration estimated from exogenous $OUR_{NH}$ and $OUR_{NO2}$ measurement, the effluent $N\text{-}NH_4^+$, $N\text{-}NO_2^-$, $N\text{-}NO_3^-$ concentration can be simulated and shown in the "Simulated 1" curves. It can be seen that the simulated curves slightly deviated from the measured values. By adjusting the $\mu_{AOB}$ value from 0.74 to 0.79 $d^{-1}$, the simulated values in "Simulated 2" curves show a better fit to the experiment data. The simulated AOB and NOB concentration using the adjusted parameter values also show a better fit to the experimental data than the original parameter (**Fig.6 (1)**). The slightly adjustment of parameter values indicated there were experiment error in the parameter estimation experiment. However, the partial nitrification can still be successfully started by using the model optimization results.

## 4. Discussion

### 4.1 Overall remarks

The full nitrification process was converted to partial nitrification with 80% nitrite accumulation rate within 10 days by using the model based optimization method. The model

with accurate parameter estimation allows for proactively intervening of the partial nitrification startup process. Given pH value of 8.2 and nitrogen load of 0.325 kg $N\text{-}NH_4^+/(m^3*d)$, the SRT and DO concentration were optimized by the model to increase the NOB washout speed while maintaining enough AOB for TAN removal.

The model optimization results in **Fig.2** show that partial nitrification can be achieved in nearly all the DO and SRT range investigated. However, process with different SRT has different required DO concentration. This suggests that the DO and SRT are interdependent factors and should not be considered alone for the partial nitrification startup. The model based approach allows the partial nitrification condition to be identified in a holistic way considering the dynamic and interdependent factors affecting partial nitrification.

### 4.2 Effect of DO on partial nitrification startup

Contrary to the reported value in some literatures [15, 21], the estimated oxygen half saturation constant for AOB was higher than NOB. However, the finding is consistent with reports by Ciudad et al.[34], who found that ammonium removal rate is dependent on the DO concentration and nitrite accumulation rate is independent on DO concentration. Both phenomena point to the conclusion that $K_{OAOB}$ is high and $K_{ONOB}$ is small. This means that partial nitrification startup will not be successful by adjusting DO alone, as the AOB is more affected by DO than NOB. Instead of producing NOB washout, the low DO technique commonly used for partial nitrification startup [8, 13] is likely to cause the washout of AOB, if NOB is not subject to other inhibition.

The suggested DO concentration by model based optimization was 0.6-0.75 mg/L under SRT of 15 days and 0.9-1.35 mg/L under SRT of 10 days. Although similar lower DO concentration was used by previous researchers [8, 13] for partial nitrification startup, the underlying mechanism were different. The low DO concentration for partial nitrification is based on the assumption that NOB has lower DO affinity than AOB, therefore the low DO could provide selective pressure on NOB for its washout[8, 13]. However, the low DO concentration used in this study was to slow down the TAN removal to increase the FA concentration for the inhibition of NOB. This mechanism is in agreement with findings by Ruiz et al. [6], who reported no partial nitrification occurred under DO concentration of 5.5 mg/L and pH values between 6.45-8.95, but achieved partial nitrification after reduced DO to 0.7 mg/L.

### 4.3 Effect of FA on partial nitrification startup

The FA was found to be effective in inhibiting NOB as indicated by the low FA inhibitive factor ($K_I$ =0.33 mg $N\text{-}NH_3$/L ), which means the growth rate of NOB reduced to half at 0.33 mg/L FA concentration. The partial nitrification startup by utilization of FA inhibition has been reported previously [20, 34]. In their studies, the pH value was adjusted online to maintain FA concentration of 3-4 mg/L and DO concentration was varied between 0.6-5.0 mg/L. In this study, by using the model based approach, the nitrite accumulation and TAN removal can be considered simultaneously in optimizing the pH, DO and SRT.

Ruiz et al. [6] have reported that pH was not a useful operational parameter for nitrite accumulation as complete nitrification of ammonia to nitrate occurred within the pH range of 6.45-8.95. This seems to contradict to the finding in this study and those reported by others [20, 34]. However, a continuous flow system with DO concentration of 5.5 mg/L was used by Ruiz et al. [6]. Under such condition, the TAN could be completely removed and FA concentration was low even under high pH of 8.95. To accumulate nitrite, the high pH should be companied by low DO in order to increase the FA concentration for NOB inhibition. By applying oxygen limitation of 1.5 mg $O_2$/L, FA inhibition under pH 7.5 and SRT of 3 days, partial nitrification was achieved by Ahn et al.[26] in a continuous flow reactor. This suggesting the adjustment pH alone is not a good practice for partial nitrification startup, which is also affected by other factors such as DO and SRT etc. The relationship among these operational parameters is highly interacting and dynamic. This makes choosing the right operation condition difficult by trial and error method. For example, the oxygen limitation can be applied to reduce TAN removal and increase FA inhibition for NOB. However, reducing the DO concentration than necessary could lead to deterioration of TAN removal. In this study, the model based optimization method was shown to be a promising technique for partial nitrification startup.

### 4.4 The effect of SRT on partial nitrification startup

A wide range of SRT from 1 to 30 days has been reportedly used for partial nitrification operation [5, 9, 18]. This suggested that the SRT alone is not a decisive factor for partial nitrification. The model based optimization results shown in **Fig.2** indicated SRT between 3-15 days can all be used for partial nitrification by adjusting the corresponding DO concentration. However, the required DO range for partial nitrification is much narrower in 15 days SRT than in 10 days SRT. This makes low SRT a preferred operation condition under the experimental condition used in this study. Furthermore, the low SRT could increase the washout speed for NOB, therefore increase partial nitrification startup speed. Pollice et al. [40] also found nitrite buildup was more significant under low SRT. On the other hand, the low SRT leads to low biomass concentration, which could cause the partial nitrification system to be instable compared to long SRT operation[9].

## 5. Conclusion

The study also suggests a new explanation for using low DO concentration to induce partial nitrification. Contrary to the commonly assumed view that AOB has higher DO affinity than NOB, the AOB was found to have a higher DO half saturation constant (lower DO affinity) than NOB in the parameter estimation experiment. The low DO concentration used in this study was to slow down the TAN removal, therefore increase the FA concentration for the inhibition of NOB.

The synergetic impact by various factors on partial nitrification can be evaluated the model based approach, by which an optimized operational condition could be calculated and enabled the conversion of the full nitrification process into a partial nitrification operation within 10 days of startup period. The costing and time consuming experiments can be circumvented in identifying the best operation strategy for partial nitrification startup by using the model based

optimization.

**Acknowledgement**

The financial support from National Natural Science Foundation of China (51478410) is highly appreciated.

## 6. Reference

1. W. Zhi, L. Yuan, G. Ji and C. He, *Environ. Sci. Technol.*, 2015, **49**, 4575-4583.
2. E. Bock, H. P. Koops, H. Harms and J. Prosser, in *Nitrification*, Oxford University Press, Oxford, 1986, pp. 17-38.
3. Y. Peng and G. Zhu, *Appl. Microbiol. Biotechnol.*, 2006, **73**, 15-26.
4. B. Sinha and A. Annachhatre, *Reviews in Environmental Science and Bio/Technology*, 2007, **6**, 285-313.
5. Q. Yang, Y. Peng, X. Liu, W. Zeng, T. Mino and H. Satoh, *Environ. Sci. Technol.*, 2007, **41**, 8159-8164.
6. G. Ruiz, D. Jeison and R. Chamy, *Water Res.*, 2003, **37**, 1371-1377.
7. S. Gu, S. Wang, Q. Yang, P. Yang and Y. Peng, *Bioresour. Technol.*, 2011, **112**, 34-41.
8. J. M. Garrido, W. A. van Benthum, M. C. van Loosdrecht and J. J. Heijnen, *Biotechnol. Bioeng.*, 1997, **53**, 168-178.
9. I. Jubany, J. Lafuente, J. A. Baeza and J. Carrera, *Water Res.*, 2009, **43**, 2761-2772.
10. D. Wei, X. Xue, L. Yan, M. Sun, G. Zhang, L. Shi and B. Du, *Chem. Eng. J.*, 2014, **235**, 19-26.
11. D. Wei, B. Du, X. Xue, P. Dai and J. Zhang, *Appl. Microbiol. Biotechnol.*, 2014, **98**, 1863-1870.
12. L. Yuan, W. Zhi, Y. Liu, S. Karyala, P. J. Vikesland, X. Chen and H. Zhang, *Environ. Sci. Technol.*, 2015, **49**, 824-830.
13. Y. Ma, Y. Peng, S. Wang, Z. Yuan and X. Wang, *Water Res.*, 2009, **43**, 563-572.
14. D. Wei, B. Du, J. Zhang, Z. Hu, S. Liang and Y. Li, *Bioresour. Technol.*, 2015, **190**, 474-479.
15. A. Guisasola, I. Jubany, J. A. Baeza, J. Carrera and J. Lafuente, *J. Chem. Technol. Biotechnol.*, 2005, **80**, 388-396.
16. B. Balmelle, K. M. Nguyen, B. Capdeville, J. C. Cornier and A. Deguin, *Water Sci. Technol.*, 1992, **26**, 1017-1025.
17. F. Cecen and I. E. Gonenc, *Water Environ. Res.*, 1995, **67**, 132-142.
18. C. Hellinga, M. C. M. van Loosdrecht and J. J. Heijnen, *Mathematical and Computer Modelling of Dynamical Systems*, 1999, **5**, 351-371.
19. A. C. Anthonisen, R. C. Loehr, T. B. Prakasam and E. G. Srinath, *J. Water Pollut. Control Fed.*, 1976, **48**, 835-852.
20. C. Antileo, A. Werner, G. Ciudad, C. Munoz, C. Bornhardt, D. Jeison and H. Urrutia, *Biochem. Eng. J.*, 2006, **32**, 69-78.
21. U. Wiesmann, *Adv. Biochem. Eng. Biotechnol.*, 1994, **51**, 113-154.
22. V. Pambrun, E. Paul and M. Sperandio, *Biotechnol. Bioeng.*, 2006, **95**, 120-131.
23. M. Mauret, E. Paul, E. Puech-Costes, M. T. Maurette and P. Baptiste, *Water Sci. Technol.*, 1996, **34**, 245-252.
24. S. Ge, S. Wang, X. Yang, S. Qiu, B. Li and Y. Peng, *Chemosphere*, 2015, **140**, 85-98.
25. V. Pambrun, E. Paul and M. Sperandio, *Chemical Engineering and Processing: Process*

*Intensification*, 2008, **47**, 323-329.

26. J. H. Ahn, R. Yu and K. Chandran, *Biotechnol. Bioeng.*, 2008, **100**, 1078-1087.
27. D. Kaelin, R. Manser, L. Rieger, J. Eugster, K. Rottermann and H. Siegrist, *Water Res.*, 2009, **43**, 1680-1692.
28. J. Wu and C. He, *Water Res.*, 2012, **46**, 3507-3515.
29. S. Chellam and M. R. Wiesner, *Environ. Sci. Technol.*, 1997, **31**, 819-824.
30. I. Iacopozzi, V. Innocenti, S. Marsili-Libelli and E. Giusti, *Environmental Modelling & Software*, 2007, **22**, 847-861.
31. P. A. Vanrolleghem, H. Spanjers, B. Petersen, P. Ginestet and I. Takacs, *Water Sci. Technol.*, 1999, **39**, 195-214.
32. J. Wu, X. Jiang and A. Wheatley, *Desalination*, 2009, **249**, 969-975.
33. M. Henze, W. Gujer, T. Mino and M. van Loosdrecht, *Activated Sludge Models: ASM1, ASM2, ASM2d and ASM3* IWA Publishing, London, 2000.
34. G. Ciudad, R. Gonzalez, C. Bornhardt and C. Antileo, *Water Res.*, 2007, **41**, 4621-4629.
35. G. Liu and J. Wang, *Water Res.*, 2012, **46**, 5954-5962.
36. R. Manser, W. Gujer and H. Siegrist, *Water Res.*, 2005, **39**, 4633-4642.
37. H. Daebel, R. Manser and W. Gujer, *Water Res.*, 2007, **41**, 1094-1102.
38. G. Munz, C. Lubello and J. A. Oleszkiewicz, *Water Res.*, 2010, **45**, 557-564.
39. I. Jubany, J. n. Carrera, J. Lafuente and J. A. Baeza, *Chem. Eng. J.*, 2008, **144**, 407-419.
40. A. Pollice, V. Tandoi and C. Lestingi, *Water Res.*, 2002, **36**, 2541-2546.

**Table 1 – Process kinetics and Stoichiometry for the two-step nitrification model**

| Components | | Components | | | | | | Reaction rate |
|---|---|---|---|---|---|---|---|---|
| | | *1* | *2* | *3* | *4* | *5* | *6* | |
| Processes | | $X_{AOB}$ | $X_{NOB}$ | $S_O$ | $S_{NO2}$ | $S_{NO3}$ | $S_{NH}$ | |
| 1 | Aerobic growth of *AOB* | 1 | | $1-\frac{3.43}{Y_{AOB}}$ | $\frac{1}{Y_{AOB}}$ | | $-\frac{1}{Y_{AOB}}-i_{XB}$ | $\mu_{AOB}\frac{S_{NH}}{K_{SH}+S_{NH}}\frac{S_O}{K_{O,AOB}+S_O}X_{AOB}$ |
| 2 | Aerobic growth of *NOB* | | 1 | $1-\frac{1.14}{Y_{NOB}}$ | $-\frac{1}{Y_{NOB}}$ | $\frac{1}{Y_{NOB}}$ | $-i_{XB}$ | $\mu_{NOB}\frac{S_{NO2}}{K_{NO2}+S_{NO2}}\frac{S_O}{K_{O,NOB}+S_O}\frac{K_I}{K_I+FA}X_{NOB}$ |
| 3 | Endog. Respiration of $X_{AOB}$ | -1 | | $1-f_p$ | | | $i_{XB}-f_p i_{XP}$ | $b_{AOB}X_{AOB}$ |
| 4 | Endog. Respiration of $X_{NOB}$ | | -1 | $1-f_p$ | | | $i_{XB}-f_p i_{XP}$ | $b_{NOB}X_{NOB}$ |

**Table 2- Kinetic and Stoichiometric parameters for the two-step nitrification model**

| No. | Symbols | Descriptions | Values | Source |
|---|---|---|---|---|
| 1 | $\mu_{AOB}$ | Maximum specific growth rate for AOB ($d^{-1}$) | 0.74 | Calibrated |
| 2 | $K_{NH}$ | Ammonium half-saturation coefficient for AOB (mg N-$NH_4$/L) | 0.51 | Calibrated |
| 3 | $K_{O,AOB}$ | Oxygen half-saturation coefficient for AOB (mg DO/L) | 1.0 | Calibrated |
| 4 | $\mu_{NOB}$ | Maximum specific growth rate for NOB ($d^{-1}$) | 0.72 | Calibrated |
| 5 | $K_{NO2}$ | Nitrite half-saturation coefficient for NOB (mg N-$NO_2$/L) | 0.49 | Calibrated |
| 6 | $K_{O,NOB}$ | Oxygen half-saturation coefficient for NOB (mg DO/L) | 0.35 | Calibrated |
| 7 | $K_I$ | FA inhibition coefficient for NOB (mg N-$NH_3$/L) | 0.33 | Calibrated |
| 8 | $b_{AOB}$ | Decay coefficient for AOB ($d^{-1}$) | 0.13 | Calibrated |
| 9 | $b_{NOB}$ | Decay coefficient for NOB ($d^{-1}$) | 0.05 | Calibrated |
| 10 | $Y_{AOB}$ | Yield for AOB | 0.20 | Calibrated |
| 11 | $Y_{NOB}$ | Yield for NOB | 0.05 | Calibrated |
| 12 | $i_{XB}$ | Mass of Nitrogen per biomass COD (gN/g COD) | 0.086 | Henze, 2000 |
| 13 | $i_{XP}$ | Mass of Nitrogen per inert particles COD (gN/g COD) | 0.06 | Henze, 2000 |
| 14 | $f_P$ | Fraction of biomass leading to particulate products | 0.08 | Henze, 2000 |

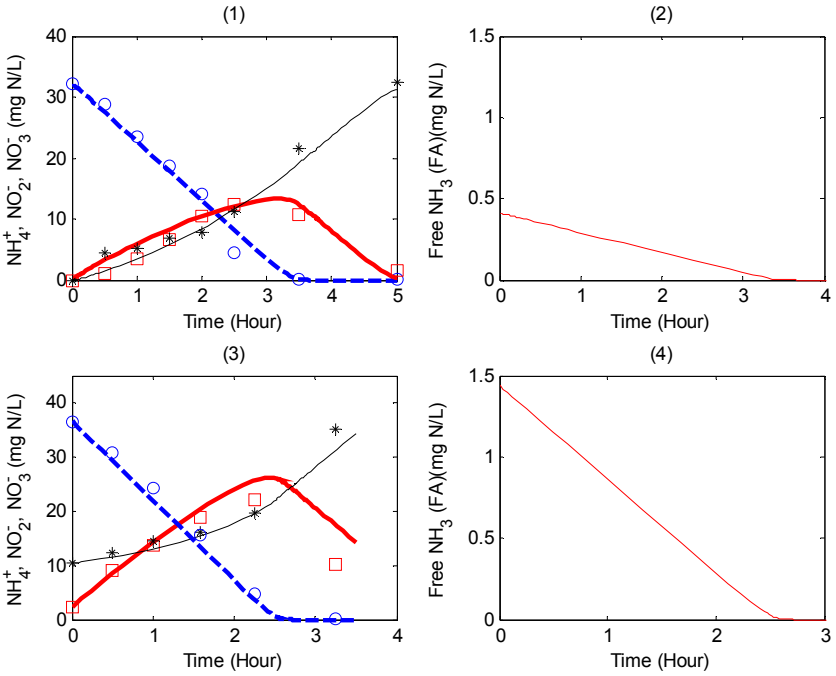


**Fig.1-** profile of N-$NH_4^+$, N- $NO_2^-$ , N- $NO_3^-$, and FA under pH of 7.5±0.1 and 8.0±0.1, other conditions remain the same

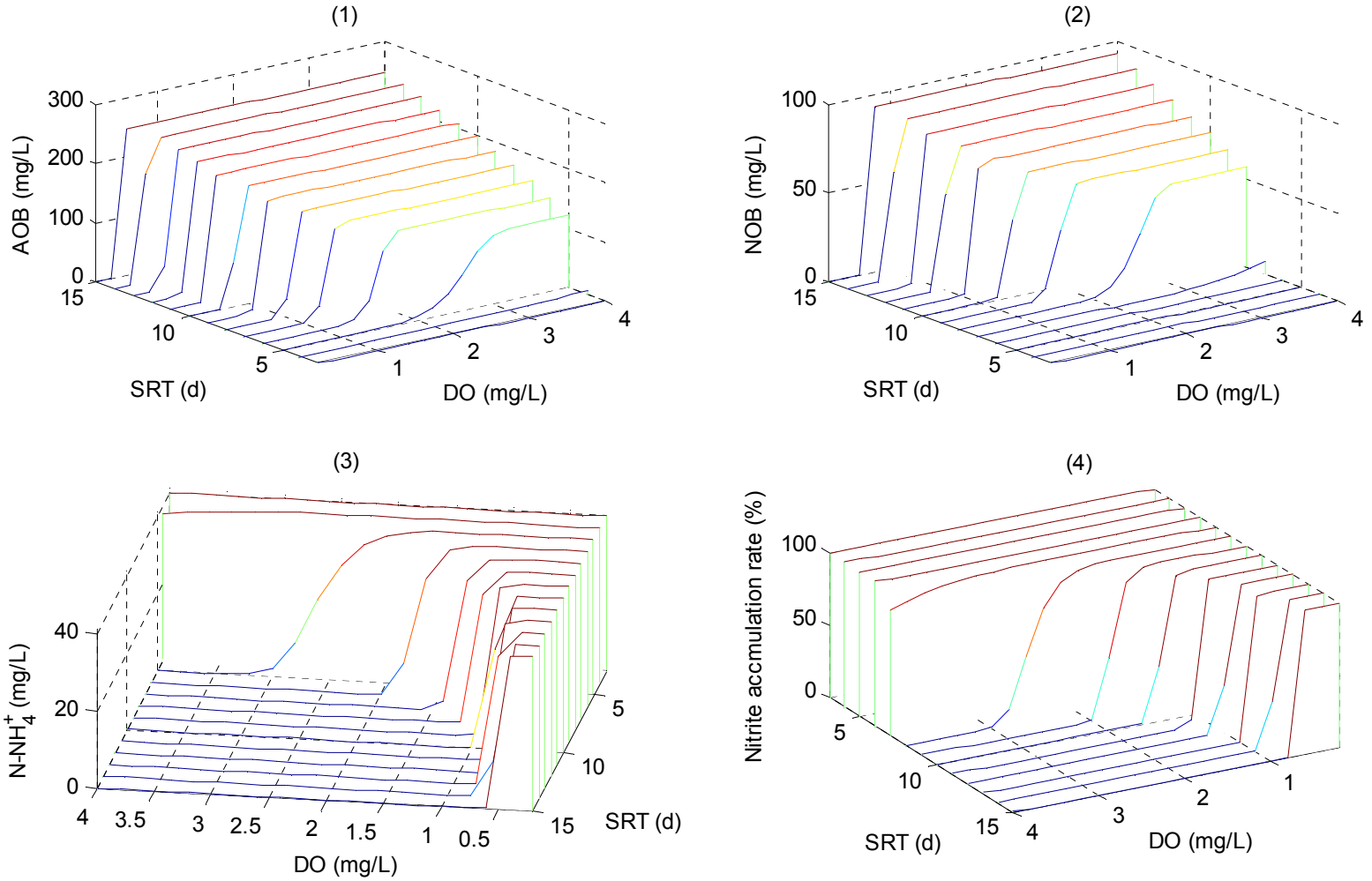


**Fig.2**- Predicted AOB, NOB, effluent concentration and nitrite accumulation rate under SRT of 3 to 15 days and DO 0.3-4.0 mg/L

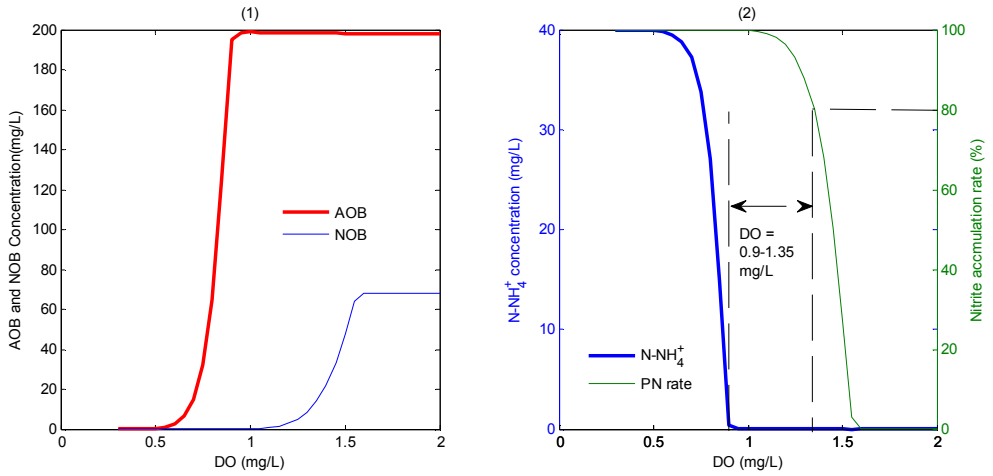


**Fig.3-** Predicted AOB, NOB, effluent concentration and nitrite accumulation rate under SRT = 10 days and DO 0-2.0 mg/L

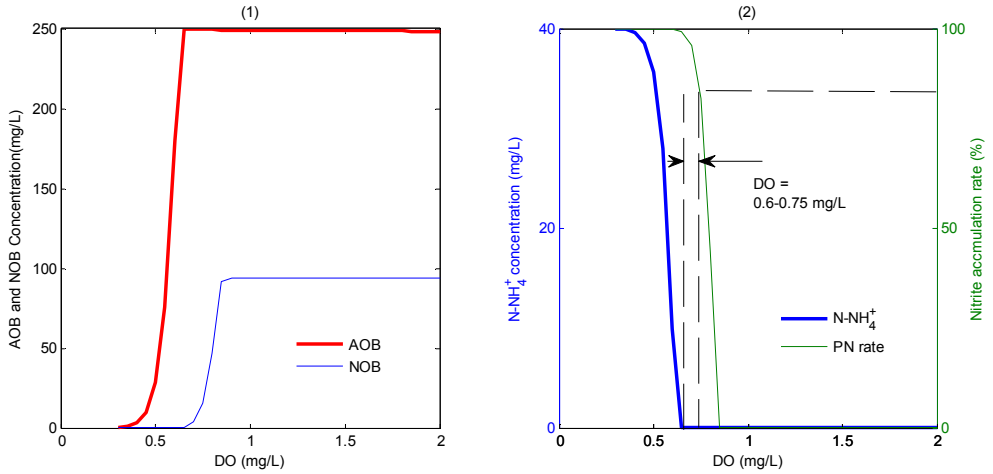


**Fig.4-** Predicted AOB, NOB, effluent concentration and nitrite accumulation rate under SRT = 15 days and DO 0-2.0 mg/L

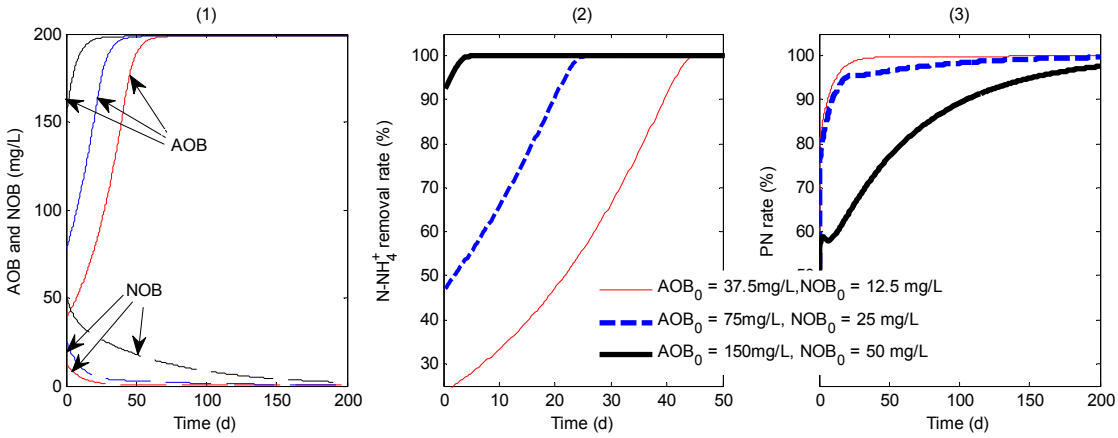


**Fig.5-** Effect of initial AOB and NOB concentration on partial nitrification performance

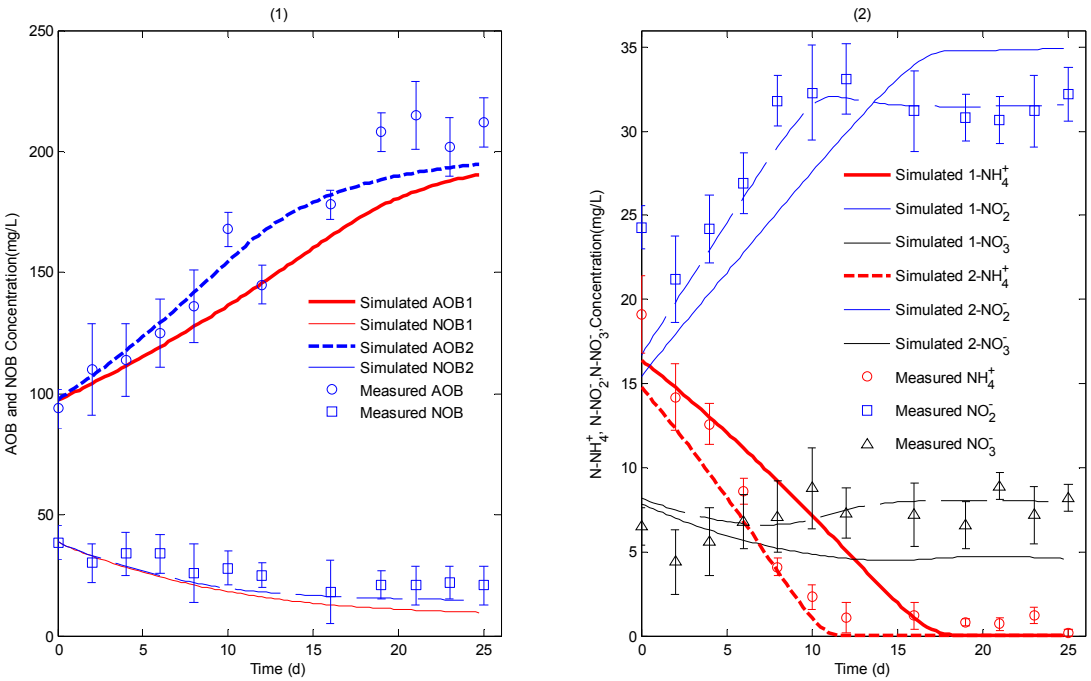


**Fig.6-** Experimental verification of the model based optimization results

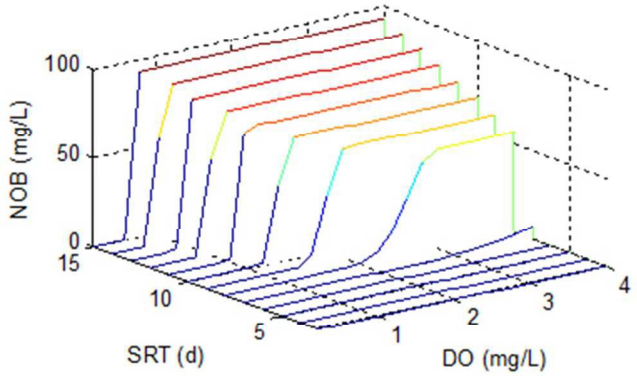


Nitrite oxidizing bacteria washout condition achieved by model based approach

211x141mm (72 x 72 DPI)